Considerations and Simulations of Subfrequency Excitation of Series Integrated Resonant Tunneling Diodes Oscillator

Runhua Sun, *Student Member, IEEE,* Olga Boric-Lubecke, *Student Member, IEEE,* Dee-Son Pan, *Member, IEEE,* and Tatsuo Itoh, *Fellow, IEEE*

Abstract— **A subfrequency pulse initiation of an oscillator of two series-integrated RTD's is considered and simulated. A voltage-dependent current source is adopted to separate the input and output power to represent a circulator in simulations. Simulations show, for example, a 100 GHz integrated RTD oscillator can be excited by a 50 GHz pulse with about 1 ns decay time (a characteristic decay time of 0.2 ns) without the dc instability problem, while a voltage ramp of 1ns rise or fall time is far too slow to initiate such an oscillator. The mechanism that RTD's are driven by subfrequency into the negative differential resistance (NDR) from the positive differential resistance (PDR) is analyzed in detail. A preliminary analysis of the transition from 50–100 GHz oscillation is also presented.**

I. Introduction

THE DOUBLE-BARRIER quantum-well resonant tunneling diode has great potential as a very high frequency solid-state oscillator. More than 700 GHz [1] of oscillation has been demonstrated by using a single quantum well resonant tunneling diode (RTD). It currently is the highest-frequency solid state oscillator. However, the reported power has been very low, often a few μwatts [1]–[3]. The series integration of RTD's for substantially more power generation is essential for many useful applications [4]. How to initiate and maintain stable oscillation in an series-connected RTD oscillator is of great interest.

It is well known that such series integration is dc unstable. The initial dc bias voltage of each resonant tunneling diode always locates in a positive differential resistance region of its I-V curve [4]. It has recently been shown by simulation that the series-connected RTD's with different dc bias voltages in the positive differential resistance (PDR) region can be driven into negative differential resistance (NDR) region and generate oscillation if the RF voltage across the series-integrated RTD's is larger than a threshold RF voltage (v_t) [5]. Experimental demonstration of the RF excitation and oscillation has been successful by using tunnel diodes [6].

In this paper, we report the theoretical consideration and the corresponding simulation of a proposed subfrequency excitation of an oscillator consisting of two series-integrated RTD's. A preliminary letter has been published [7]. Since the proposed scheme is relatively unknown to the microwave community, and many things are left unclear in a letter-form presentation, a more detailed presentation is provided here. In this new scheme, the series-integrated RTD's are driven into the NDR region by a pulsed RF source at a substantially lower frequency. Theoretical considerations suggest that the RTD's in the PDR region can be driven to the NDR region by a lower frequency source and the oscillation at the higher fundamental frequency can be initiated and eventually dominates the oscillator circuit when the lower frequency source is turned off. Computer simulation for this proposed scheme is carried out for a number of cases. The results are very encouraging. For example, a simulated 100 GHz integrated RTD oscillator can be readily induced into oscillation by a 50 GHz pulse with about 1 ns decay time (a characteristic decay time of 0.2 ns). It is known [4] that a voltage ramp of a rise or fall time of even 30 times shorter than 1 ns is still too slow to initiate such an oscillator. To our knowledge, the proposed scheme has not been reported in any electronic systems. Preliminary experimental demonstration of this subfrequency excitation induced oscillation by tunnel diodes at much lower frequencies has also been successful [8].

The preliminary demonstration of the scheme may lead to many practical applications for N series-connected quantum-well RTD's in the millimeter-wave and submillimeter-wave frequencies. Based on this device-level integration, further circuit-lever integration can be achieved. One implication is that when implemented with quasi-optical multiplier-type of circuits [9], useful power well into millimeter and submillimeter waves can be generated by integrated RTD's. Note that circulator is not required in such multiplier type circuits.

This paper is organized as follows. The theoretical considerations are presented in Section II. The simulation results are presented and discussed in Section III. The conclusion is in Section IV.

II. Theoretical Considerations

The small reported power of a single RTD oscillator is mainly due to its low device impedance [2]. Therefore, series integration of RTD's is a very desirable start for power enhancement. Due to the severe ohmic loss (even for metal) at millimeter and submillimeter wave frequencies, device level

Manuscript received January 30, 1995; revised June 29, 1995. This work was supported by the UCLA Joint Service Electronics Program.

The authors are with the Electrical Engineering Department, University of California, Los Angeles, CA 90024 USA.

IEEE Log Number 9414235.

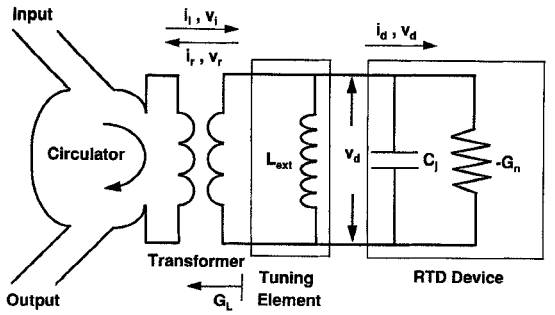

Fig. 1. A schematic circuit diagram for subfrequency pulse excitation of an oscillator of series integrated RTD's. A circulator is used here to separate input and output. If in a quasi-optical arrangement, the circulator is not required.

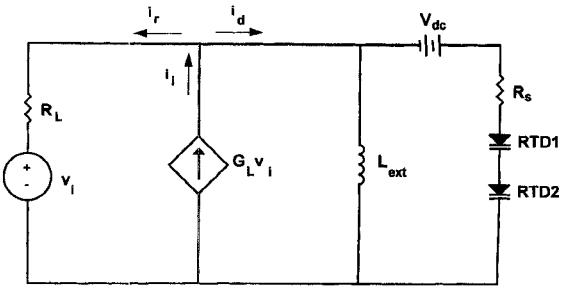

Fig. 2. A convenient equivalent circuit model to separate input and output power of the integrated oscillator circuit of Fig. 1.

integration is very important. It provides a solid foundation for further circuit level integration.

A well-known dc instability problem poses a difficulty for series integration of any diodes exhibiting NDR [10]. RTD's, like tunnel diodes, have their NDR derived directly from their dc I-V characteristics. Even though transit time effect is presented in RTD [4], it does not change the aspect of the dc instability. One way to circumvent this difficulty was proposed and demonstrated experimentally by Vorontsov and Polyakov [10]. A voltage shock wave was applied to ten tunnel diodes to drive the bias voltage of every diode into the NDR region to initiate oscillation. The oscillation is then stabilized by designing the resonant circuit to give a large RF voltage amplitude [10]. The RF performance of the series-integrated RTD devices used as millimeter-wave oscillator through a shock-wave stabilization scheme has been theoretically investigated [4]. In that investigation the GaAs nonlinear transmission line (NLTL) [11], was proposed as a fast switch to turn on the dc bias in a picosecond range to initiate a high frequency oscillation. As mentioned earlier, another initiation scheme by using a pulsed source such as an IMPATT diode to excite the oscillator was also proposed and theoretically investigated [5]. In this scheme, the oscillation was initiated by an input pulsed power which can be injected into the oscillator [5]. Note that the mechanism of the drive-in by a shock wave or NLTL is entirely different from that by a RF voltage.

In this work, we consider excitation of the series integrated RTD oscillator by using a RF pulse at lower frequency. There are many solid state sources at lower end of millimeter wave frequencies. As will be shown later, the pulse duration is of the order of nanoseconds. Therefore it is easier to implement. Furthermore, the scheme may be repeated to reach higher and higher frequencies.

A schematic diagram for a simplest circuit of such purpose is shown in Fig. 1. This circuit is the same as was used in [5]. Note that a multiplier-type of circuit can be used to enhance the coupling efficiency, which we have not done here. Furthermore, when quasi-optical circuits are used, input and output are separated without the requirement of a circulator [9].

Berkeley SPICE is used in our simulations. Fig. 2 is the equivalent circuit model that we invent to represent Fig.1 in SPICE. Two RTD's are used here to demonstrated the scheme. The equivalent load admittance seen from the device terminals is represented by $Y_L = G_L + 1/j\omega L$. The equivalent voltage and current components of the incident and the reflected waves are represented by v_i, i_i, v_r, and i_r, where the subscripts i and r, respectively, refer to the incident and reflected waves. The crux in the equivalent circuit is how to separate the input and output of Fig. 1. Even with the modified version of Microwave SPICE, an element such as a circulator is not available. We have overcome this difficulty by adopting a clever dependent current source as shown in Fig. 2. In terms of incident and reflected voltages, the device terminal voltage is given by

$$v_d = v_i + v_r. \tag{1}$$

Similarly, the device terminal current is

$$i_d = i_i - i_r = G_L(v_i - v_r). \tag{2}$$

In Fig. 2 the input voltage is represented as an independent voltage source in series with the load resistance R_L, where the R_L is the reciprocal of the G_L of Fig. 1. The dependent current source $G_L v_i$ gives the input current i_i in Fig. 1. The reflected current i_r in Fig. 1 is represented by the current of the branch with the v_i source. It is then straightforward to show that the device current i_d and voltage v_d in Fig. 2 relates the input and output currents and voltages in exactly the same fashion as (1) and (2).

In this work, we consider only the simple case of two series-connected RTD's. Our equivalent circuit consists of two series-connected RTD's, a series resistance, a load resistance, a dc bias voltage, a tuning inductance, an input voltage source, and a voltage-controlled current source. Each of two active devices is assumed to be a capacitance in shunt with a nonlinear conductance defined by the I-V curve of the RTD. We treat the capacitance as a constant because it does not vary much, only 10–20% even for large RF voltage amplitude [12]. The tuning inductance is for canceling the capacitive component of the RTD's impedance at the fundamental frequency. A series resistance R_s accounts for the resistance of the bulk semiconductor and ohmic contacts, and is not a function of the voltage across the device [12].

How to represent the I-V characteristic of a resonant tunneling diode in SPICE simulation is another problem. The experimental dc I-V curve of [13] is used in our work. An analytical expression of the I-V curve is preferred. We first tried the formula used for tunnel diode [14]. No satisfying fitting can be produced. Physically, this is because the mechanisms

of these two devices are vastly different. We have also tried to adopt the formula by Chang *et al.* [15]

$$I = f\{C_1^* V[\tan^{-1}(C_2^* V + C_3) - \tan^{-1}(C_2^* V + C_4)] + C_5^* V^m + C_6^* V^n\}, \quad (3)$$

where f and $C_1, C_2, C_3, C_4, C_5, C_6, m, n$, are the constants determined by device properties. The best fittings are still not satisfactory, particular in the negative resistance region which is crucial in our simulation. We finally adopt a linear piece-wise fitting to represent the I-V curve. The option in SPICE for transcendental forms of voltage-controlled current sources and switches are used to implement the piece-wise function. The fittings are plotted in the Fig. 3, in which dashed line is measured data, the dotted line is based on (3), and solid line is the linear piece-wise fitting used in our simulation. The fitting results by using the formula for tunnel diodes are not shown because the disparity is large. In the simulation that will be reported next, we find it is always possible to drive the series connected RTD's from PDR region to NDR region even by lower frequency RF source as long as the amplitude is sufficiently large. A preliminary account of this scheme has been given in [8]. The following theoretical arguments and derivations will support them. In Fig. 2, the dc voltage source is intended to bias the both diodes in the middle of the NDR region. Due to dc instability, initially one diode is biased on the first rising branch of the dc I-V curve, whereas the other one is biased on the second rising branch. The two diodes have same conductive current, and no capacitive current. The sum of dc voltage biased on the both diodes is the applied dc voltage. Without the RF voltage across the RTD's we have

$$I_{R1} = I_{R2}, \quad (4)$$

$$i_{c1} = i_{c2} = 0, \quad (5)$$

$$V_{D1} + V_{D2} = V_D \quad \text{and} \quad V_{D1} \neq V_{D2} \quad (6)$$

here the I_{R1}, I_{R2}, and i_{c1}, i_{c2} is the conductive current and capacitive current in the first and second RTD, respectively. V_{D1} and V_{D2} presents the dc voltage biased on the first and second RTD. V_D is the applied dc voltage. After the RF voltage signal turns on

$$i_{T1}(t) = C\frac{dv_1(t)}{dt} + I(v_1(t)), \quad (7)$$

$$i_{T2}(t) = C\frac{dv_2(t)}{dt} + I(v_2(t)), \quad (8)$$

$$v_T(t) = v_1(t) + v_2(t), \quad (9)$$

$$v_1(t) = V_{D1} + A_1^{\mathrm{RF}} e^{jw_i t} + (\text{harmonic components}), \quad (10)$$

$$v_2(t) = V_{D2} + A_2^{\mathrm{RF}} e^{jw_i t} + (\text{harmonic components}), \quad (11)$$

$$i_{T1}(t) = i_{T2}(t) \quad (12)$$

where $i_{T1}(t), i_{T2}(t), I(v_1(t)), I(v_2(t))$, and $v_1(t), v_2(t)$ are the two total currents, two conductive currents and the two voltages of the first and second diode, respectively, and $v_T(t)$ is the total voltage across the two RTD's. The $V_{D1}, V_{D2}, A_1^{\mathrm{RF}}$ and A_2^{RF} are allowed to be slowly varying functions of time

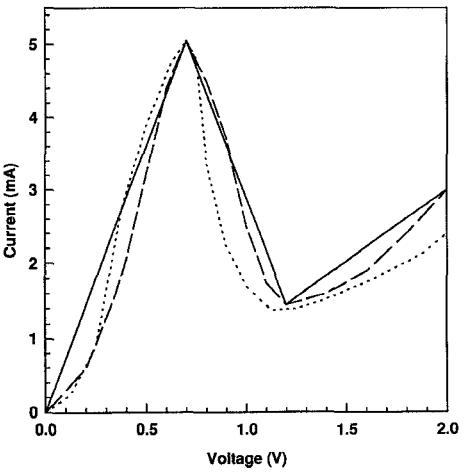

Fig. 3. The fittings comparisons of the I-V characteristic of a RTD The dashed line is the experimental data. The solid line is our linear piece-wise fitting. The dotted line is the best fitting by (4).

in (10) and (11). The ω_i is the frequency of the injected excitation pulse. As is commonly done in nonlinear analysis, the harmonic components are assumed small. Note that later, one of the harmonics may develop into the oscillation frequency. But for now, we only consider the excitation drive-in process. For the convenience of describing the motion of the bias points into the NDR region, the dc components of the current and the voltage is defined in such a way that within one RF period of ω_i the change is very slow, and can be evaluated for only one period. Using overhead bar as the notation for taking the average voltage and current over one period we get from (9) that

$$\overline{v_1(t)} + \overline{v_2(t)} = V_D. \quad (13)$$

Assuming the period averaged quantities change slowly from one period to next period, we can have

$$\frac{d\overline{v_1(t)}}{dt} + \frac{d\overline{v_2(t)}}{dt} = 0 \quad (14)$$

where the time derivative is a convenient short-hand notation. It is obtained by interpolating the difference equations into the derivative. Since i_{T1} equals i_{T2} in a series connection, therefore from (7) and (8), we have

$$\overline{C\frac{dv_1(t)}{dt} + I(v_1(t))} = \overline{C\frac{dv_2(t)}{dt} + I(v_2(t))}, \quad (15)$$

$$C\frac{d\overline{v_1(t)}}{dt} + \overline{I(v_1(t))} = C\frac{d\overline{v_2(t)}}{dt} + \overline{I(v_2(t))}, \quad (16)$$

$$C\frac{d\overline{v_1(t)}}{dt} + \overline{I(v_1(t))} = C\frac{d\overline{v_2(t)}}{dt} + \overline{I(v_2(t))}, \quad (17)$$

$$C\left(\frac{d\overline{v_1(t)}}{dt} - \frac{d\overline{v_2(t)}}{dt}\right) = \overline{I(v_2(t))} - \overline{I(v_1(t))}. \quad (18)$$

Substituting (14) into (18), we have

$$\frac{d\overline{v_1(t)}}{dt} = \frac{1}{2C}(\overline{I(v_2(t))} - \overline{I(v_1(t))}) \quad (19)$$

or, we may put in difference form

$$\Delta\overline{v_1(t)} = \frac{1}{2C}(\overline{I(v_2(t))} - \overline{I(v_1(t))})\,\Delta T. \quad (20)$$

$\overline{v_1(t)}$ and $\overline{v_2(t)}$ are the pseudo dc voltages (defined as averaging over one period) of the diode one and two, and $\overline{I(v_1(t))}, \overline{I(v_2(t))}$ is the pseudo dc current in the first and second diode, respectively, over one period, and ΔT is one period length. The (19) or (20) is the key to analyze the drive-in process. From them we see that the pseudo dc current difference between two RTD's forces the dc biased voltages of two RTD's to shift. This shift will not stop until two RTD's have the same pseudo dc current. Therefore, it is possible that the pseudo dc voltages of the two RTD's stay separately between the peak and the valley voltage of the dc I-V curve once both diodes attain the same pseudo dc bias current. The motion of the pseudo dc voltage, as shown in (19) or (20) is determined by both the "instantaneous" values of the pseudo dc voltage $\overline{V_{D1}}$ and $\overline{V_{D2}}$ as well as the pseudo RF voltage $\overline{A_1^{\mathrm{RF}}}$ and $\overline{A_2^{\mathrm{RF}}}$. The pseudo RF voltage can be obtained by the pseudo impedance $\overline{Z_1}$ and $\overline{Z_2}$ of the two diodes, which can be written as

$$\frac{1}{Z_1} = G_1(V_{D1}, \overline{A_1^{\mathrm{RF}}}) + j\omega_i C, \tag{21}$$

$$\frac{1}{Z_2} = G_2(V_{D2}, \overline{A_2^{\mathrm{RF}}}) + j\omega_i C. \tag{22}$$

An algorithm can be programmed to calculate the motion of the bias points according to (20)–(22).

The RF instability of the dc stable bias points can therefore be understood as follows: If the RF voltage of the two RTD's is not large enough, then the RF voltage apportioned to any RTD can not drive it into the negative differential resistance (NDR) region in the linear piece-wise approximations. The period average currents of the two diodes in (20) will become the same before the pseudo dc bias points move into NDR region. When the RF voltage for one of the two RTD's gets into the NDR region high order harmonics (referring to the excitation frequency ω_i) are generated. The pseudo dc current of the RTD is also changed, In the single frequency approximation the new dc current of the both RTD's can be easily evaluated for one period. The pseudo dc bias voltage shifts are then easily calculated by using (20). Therefore, the new bias points can be found one period after one period. It turns out that a RTD initially biased on the second PDR region has a larger pseudo dc current than a RTD initially biased on the first PDR region as long as the RF voltage is sufficiently large. If the RF voltage across the RTD's is greater than the threshold voltage v_t, the two RTD's will eventually biased to a converged point in the NDR region. From this kind of drive-in algorithm we can predict the threshold RF voltage across the RTD's for a given I-V curve, applied dc voltage, capacitance, etc. It is also noticed that the ΔT in (20) depends on the frequency of the injected voltage pulse. Therefore, different injected frequencies may have different threshold voltages.

The next important question is whether the oscillation can be built up and sustained when the subfrequency excitation pulse is turned off. We may analyze the situation as follows. If we treat the total conductance $-G_n$ of the series integrated RTD as a time dependent function, then the circuit behavior can be predicted if the $-G_n$ function is given. We have analyzed the problem when the input frequency is close to the oscillator frequency and found that indeed this could be done [5]. Now with subfrequency excitation, we may view the problem in this way. Initially $-G_n$ is positive, i.e., dissipative, because the individual RTD are in PDR region. A large enough RF voltage drives the RTD's into NDR regime and $-G_n$ becomes negative, i.e., generative even at fundamental frequency of the oscillator circuit. This $-G_n$ will amplify the circuit fundamental frequency, which appears as a harmonic component first when referenced with expect to the excitation frequency. When the excitation pulse begins to decay, the $-G_n$ may further increase because the initial RF amplitude can be made larger than that of the maximum $-G_n$. Thus while the excitation RF voltage dies down to a certain level, the circuit fundamental has a chance to quickly shoot up and maintain its oscillation. Such a linearized picture is well known in multiple periodic nonlinear system [16]. The effective conductance for each harmonic of a two-frequency dominant system can be obtained by a double Fourier integral [16]. While we will work out an analytic theory in more detail, we report first in the following section, the successful computer simulation of the subfrequency excitation scheme.

III. Simulation and Results

Using Fig. 2 for simulation, we assume that the oscillator is initiated by a simple sinusoidal voltage. The free-running oscillation frequency of the equivalent circuit is designed to 100 GHz. The maximum $-G_n$ is found to be about 3.6 mS by using the linear piece-wise fitting as shown in Fig. 3. A constant capacitance is used for each RTD with value 0.02 pF as used in [13]. In order to guarantee that the RF voltage across the two series-connected RTD device is larger than the cutoff voltage [4], the load conductance is designed to 1mS in our present work. The dc applied voltage is set such that the two RTD's will be biased in the middle of NDR region after drive in. The smallest amplitude of the voltage pulse which could drive the RTD's into the NDR region at different frequencies, and the corresponding the amplitude of the RF voltage across the two RTD's after drive-in are simulated by SPICE. The results of the simulation are summarized in Fig. 4. It shows that when the excitation frequency is away from fundamental frequency of the oscillator the smallest RF voltage required to drive in increases due to the resonant nature of the circuit. However, the corresponding RF voltage across the two RTD's decreases as shown in Fig. 4. The reason for this decrease is that the ΔT in (20) is larger for low frequency than it for high frequency. Hence for the same Δv_1 (or Δv_2) the required RF voltage across the RTD's is smaller for lower frequency according to (20).

After extensive simulations, we find that it is indeed possible to drive RTD's from PDR into NDR to excite oscillation if the frequency of the input signal is not too low and the RF voltage of input pulse is large enough. In Fig. 5, we present the simulation results for the 50GHz pulse excitation. Initially, the first RTD is biased at the dc voltage 1.64 V and the second one is biased at 0.32 V. Both RTD's have the same dc bias current of about 2.3 mA. As shown in Fig. 5, the V_P and V_V of the dc I-V curve are 0.7 and 1.2 V, respectively. The

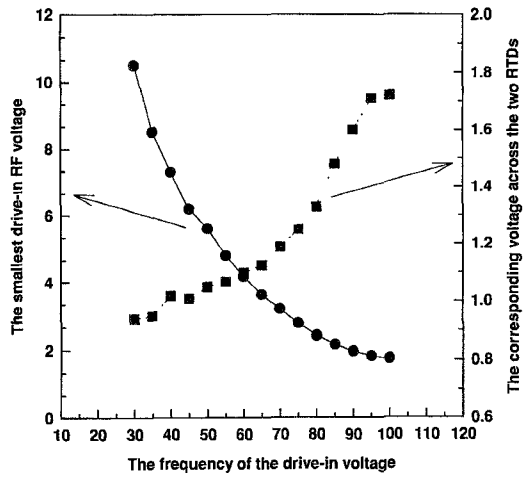

Fig. 4. The smallest RF voltage amplitudes of the input pulse to drive two RTD's from PDR region to NDR region versus the subfrequency. The circles represent the input voltage amplitude and the squares are for the corresponding voltage across the two RTD's.

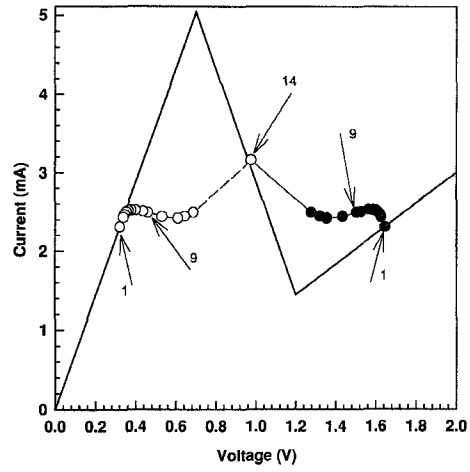

Fig. 5. The 14 simulated finally steady dc bias points of the two RTD's corresponding to different RF voltages across the two RTD's. The first point marked 1 at the original dc bias corresponds to v_{rf} below 0.76 V. Then starting from $v_{rf} = 0.8$ V in 0.02 V increment to 1.02 V, the dc bias moves toward the NDR region. The final point marked by 14 in the NDR region is the result of applying the critical voltage v_{rf} =1.04 V.

simulation shows that the dc bias points of two RTD's have no change if the amplitude of the RF voltage across the two RTD's oscillator is less than about 0.76 V. This situation is presented by the open circle and the shaded circle located at the original bias points. The difference between 0.32 and 0.7 V is 0.38 V, and between 1.64 and 1.2 is 0.44 V. It turns out to be a good approximation to assume that both RTD's equally share the total RF voltage across them. In the linear piece-wise fitting, we would expect the bias points begin to shift according to (20) only when the total RF voltage is greater than 0.76 V, i.e., twice of 0.38 V. When the amplitude of the RF voltage across the RTD's is changed from 0.8–1.02 V with 0.02 V increment the final steady state dc bias points of two RTD's are shifted gradually toward the middle of the NDR region, but do not come into the NDR region as shown in Fig. 5. As the RF voltage across the two RTD's reaches 1.04 V the dc bias points of the both RTD's are suddenly pulled to the middle of the NDR region and converged to one point. When the RF voltage across the two RTD's is above the 1.04 V the steady dc bias points of the two RTD's are always stabilized in the NDR region of the I-V characteristic. Therefore, in this case, 1.04 V is the critical RF voltage that the two bias points in the PDR region exhibit a RF instability, in the sense that those dc stable bias points will become RF unstable. The converged bias point in the NDR region is dc unstable that is RF stable when the RF voltage is larger than the critical voltage.

We have further investigated the transient behavior of the two critical situations that the RF voltage across the two RTD's are 1.02 and 1.04 V. The transient response of the dc bias points corresponding to these two conditions are simulated. Fig. 6 shows the transient response of the dc bias points by applying 1.02 V RF voltage across the RTD's and Fig. 7 shows the case of 1.04 V RF voltage. In these two figures, each circle presents the result of the time increment of one period (0.02 ns). The shade circles present the transient response of the first RTD and the open circles present the transient response of the second RTD. As shown in Fig. 6 the dc bias points are driven toward the middle of the NDR region period by period. After about 25 periods both RTD's come to the same dc bias current so that a steady state is attained. This can be easily understood by (20). Although the dc bias points of two RTD's have been pushed hard toward the NDR region, the final biased points are not converged into the NDR region because the RF voltage across the RTD's (1.02 V) is still not large enough. On the other hand, in Fig. 7 we see that 1.04 V is just sufficient to drive the two RTD's from initial bias points to the middle point of the NDR region. We have checked that in Figs. 6 and 7, the shifts of the dc bias voltages of the each RTD are proportional to the difference of the dc bias current at the end of each period as shown in (20). In the first several periods or just before the final drive-in the dc bias voltages of the two RTD's are shifted more due to a larger difference between the pseudo dc currents of the two RTD's. We also find that if the RF voltage across the RTD's is larger, then the process of the drive-in is faster. All these simulation results are in good agreement with our analysis in (20).

Some general trend can be said about what kind of I-V curve has a advantage for drive-in. For example, if the slope of the first rising branch of the I-V curve is lowered and the slope of the second rising branch is raised, then the difference of the pseudo dc currents of the two RTD's in each period will be increased. Therefore, the RTD's will be driven faster into the NDR region. Also, the pulse excitation power (or the RF voltage across the RTD's) required to drive RTD's into NDR region can be reduced by adjusting the I-V curve. To illustrate this, in Fig. 8 the solid line shows the experimental I-V curve [13] in the liner piece-wise approximation. We keep the first PDR and NDR region unchanged, but lower the slope of the second PDR from 1.95 to 0.7, which is presented by dotted line. We can also raise the slope of the second PDR to 7.2 which is shown by the dash line. By using the dash I-V curve the critical RF voltage across the RTD's required to drive them into the NDR region decreases from 1.04–0.79 V. On the other hand, the critical RF voltage rises to 1.11 V when dotted I-V curve is applied.

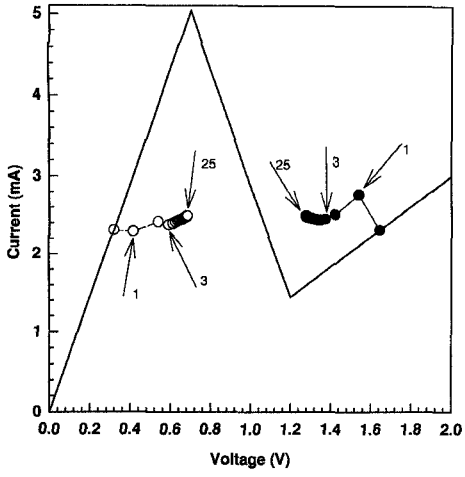

Fig. 6. The successive motion of the transient response of the pseudo dc bias points of the two RTD's by applying (50 GHz) 1.02 V RF voltage across them. Each point is the average of the voltage and current of one RTD over one period (0.02 ns). After 25 periods, the bias points stabilize themselves at the points marked by 25.

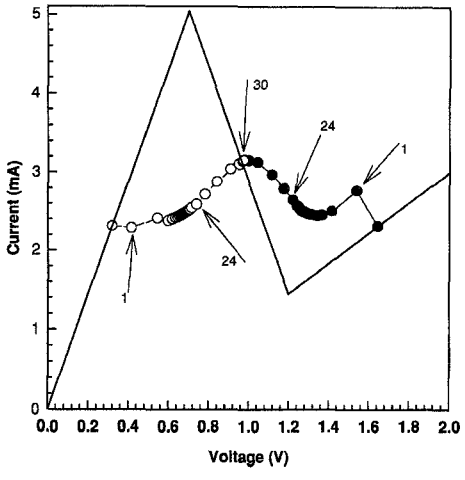

Fig. 7. Similar plot as Fig. 6, by with 1.04 V critical voltage applied. The successive motion of the two bias points finally converge to the RF stabilized bias point as marked by 30, in the NDR region.

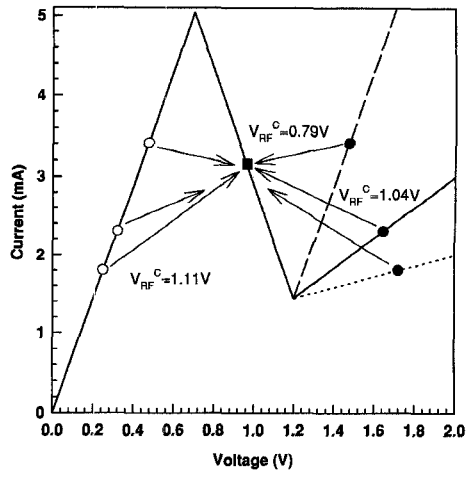

Fig. 8. Illustration of the effect of the shape of the I-V curve on the RF instability. Three slopes of the second rising branch of the I-V curve are used in the simulations. The required critical RF voltages are 0.79, 1.04, and 1.11 V as shown.

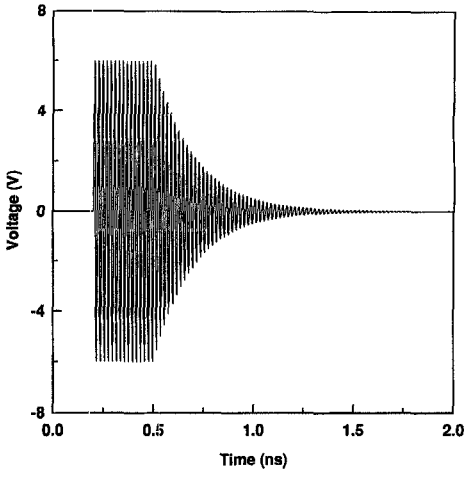

Fig. 9. The voltage of a 50 GHz excitation pulse is shown. The pulse decays exponentially with a 0.2 ns characteristic time. Other pulse shapes have also been used in our simulation with similar results.

After driving the RTD's into the NDR region the input pulse should be damped out in order to generate the 100 GHz free-running oscillation. Fig. 9 presents an example of a 50 GHz voltage pulse with 6V amplitude, which exponentially damps out by 0.2 ns characteristic time. It approximately decays to zero after 1 ns. The transient response of the voltage across the each of two RTD's by using this input pulse is plotted in Fig. 10 where the first RTD's transient response is presented by the solid curve and second RTD's is given by the dotted curve. As shown, before 0.2 ns two RTD's having different dc bias voltage are located in the first and the second PDR region, respectively, due to the dc instability. The dc bias voltages of these two RTD's are driven into the NDR region very quickly after input sinusoidal voltage is injected at 0.2 ns. The drive-in procedure takes only about 5 periods (0.1 ns) because the RF voltage across the two RTD's corresponding to the 6 V voltage pulse is about 1.14 V which is much large than the critical voltage 1.04 V. After driven in each of two RTD's shares equally the same RF voltage and dc bias voltage in the NDR region. It can be clearly seen in Fig. 10 that the oscillator maintains oscillation at about 100 GHz after the 50 GHz input pulse completely damps out. Once driven into the NDR region, two RTD's stay in the same dc bias point (in the middle of the NDR) even when the 50 GHz oscillation makes the transition to 100 GHz. The current through the oscillator in the transition region from 50–100 GHz is presented in Fig. 11. As shown, the transition from 50 GHz oscillation to 100 GHz completes near about 0.85 ns. The 100 GHz begins as a small harmonic component. It then grows in a time scale of about 0.2 ns to full strength and dominates the oscillation. In Fig. 12, the total voltage across the RTD's in the transition region is shown. The substantial growth of the 100GHz oscillation begins around 0.65 ns in Fig. 12, where the RF voltage amplitude for each RTD is about 0.25 V. Note that 0.5 V is the range of the DNR region of the experimental I-V curve. Therefore, the effective negative resistance $-G_n$, grows to a maximum when the RF pulse is decayed to that of 0.65 ns. Note that also transit time effects for $-G_n$ have been shown to be negligible at these frequencies [4]. For much higher frequencies, it should be included as discussed in [4].

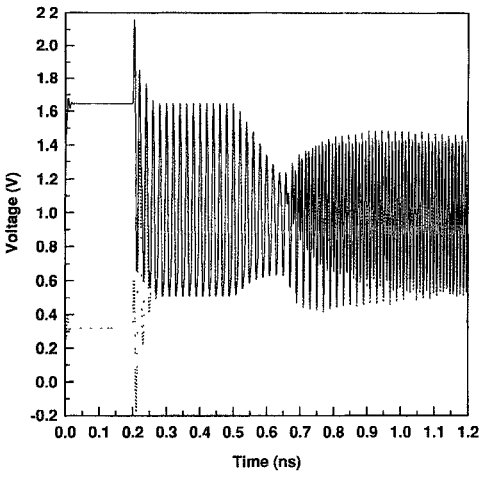

Fig. 10. The two voltages across each of the two RTD's during the drive-in period and the transition from 50 GHz into 100 GHz period with an excitation pulse shown in Fig. 9.

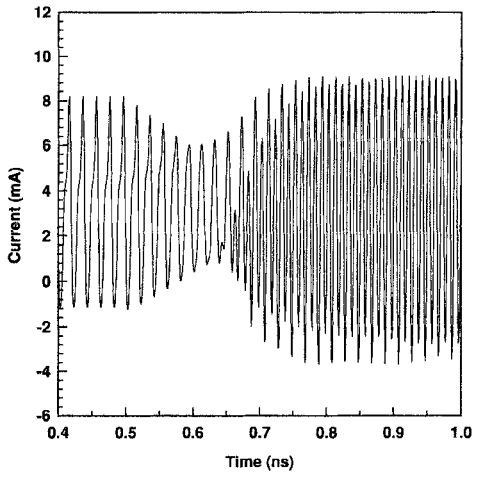

Fig. 11. The current through the two RTD's in the critical transient region in which the transition from 50–100 GHz occurs.

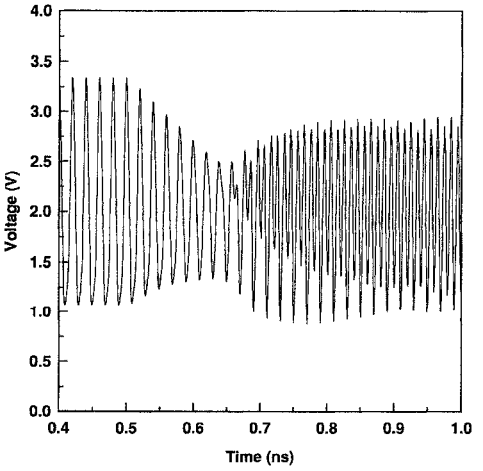

Fig. 12. The total voltage across the two RTD's in the critical transient region in which the transition from 50–100 GHz occurs.

In the simulations, we find that if the input voltage damps out too slow, then the generation of the 100 GHz oscillation may fail. It is important to note that a 50 GHz injected pulse with 1 ns decay time is able to excite a 100 GHz integrated RTD oscillator. It is impossible for a 1 ns voltage ramp to do the same thing [4]. The reason is that for our excitation scheme, the 100 GHz harmonic is already there and quickly build up in about 0.2 ns when the 50 GHz pulse decays. On the other hand, in a voltage ramp excitation, the 100 GHz must build up from noise for the whole 1ns period, which is too long to prevent switching of the bias of each RTD [4]. In fact, 1 ns voltage ramp is far too slow for such an excitation [4]. This is an important advantage of the subfrequency excitation scheme.

IV. Summary

An equivalent circuit of a simplified circulator-coupled RTD oscillation circuit model is derived and used in our simulations by SPICE. The mechanism of inducing a dc sustained high frequency oscillation of an oscillator with series-integrated RTD's by a subfrequency excitation pulse is considerated and simulated in this work. The principle of driving the RTD's from PDR region into NDR region is also analyzed and confirmed by simulations. We have presented a preliminary analysis of the transition from subfrequency to high frequency oscillations. It is demonstrated by simulations that the subfrequency pulse initiation of an oscillator of series integrated RTD's is a convenient way to circumvent the dc instability problem. Preliminary experimental demonstration of this mechanism by series-integrated tunnel diodes has been successful. Theoretical consideration shows that the mechanism can be used to millimeter wave and submillimeter wave frequencies.

References

[1] E. R. Brown, J. R. Soderstrom, C. D. Parker, L. J. Mahoney, K. M. Molvar, and T. C. McGill, "Oscillations up to 712 GHz in InAs/AlSb resonant-tunneling-diodes," *App. Phys. Lett.*, vol. 58, pp. 2291–2293, May 1991.

[2] V P. Desan, A. Mortazawi, D. R. Miller, V. K. Reddy, D. P. Neikirk, and T. Itoh, "Microwave and millimeter-wave QWITT diode oscillators," *IEEE Trans. Microwave Theory Tech*, vol. 37, pp. 1933–1941, Dec. 1989.

[3] H. Gronqvist, A. Rydberg, H. Hjelmgren, H. Zirath, E. Kollerg, J. Soderstrom, and T. Anderson, "A millimeter wave quantum well diode oscillators," in *Proc. 18th European Microwave Conf.*, Stockholm, Sweden, Sept. 1988, pp. 370–375.

[4] C. C. Yang and D. S. Pan, "Theoretical investigations of a proposed series integration of resonant tunneling diodes for millimeter-wave power generation," *IEEE Trans. Microwave Theory Tech.*, vol. 40, pp. 434–441, Mar. 1992.

[5] ——, "A theoretical study of an integrated quantum-well resonant tunneling oscillator initiated by an IMPATT diode" accepted by *IEEE Trans. Microwave Theory Tech.*, vol. 43, pp. 112–118, Jan. 1995.

[6] O. Boric-Lubecke, D. S. Pan, and T. Itoh, "RF excitation of an oscillation with several tunneling devices in series." *Microwave and Guided Wave Lett.*, vol. 4, no. 11, pp. 364–366, Nov. 1994.

[7] R. Sun, D. S. Pan, and T. Itoh, "Simulation fo a subharnomic excitation fo series integrated resonant tunneling diodes," *IEEE Microwave and Guided Wave Lett.*, vol. 5, no. 1, pp. 18–20, Jan 1995.

[8] O. Boric-Lubecke, D.-S. Pan, and T. Itoh, "Fundamental and subharmonic excitation for an oscillator with several tunneling diodes in series," accepted for publication in *IEEE Trans. Microwave Theory Tech.*

[9] W. W. Lam, C. F. Jou, N. C. Luhmann, Jr., and D. B. Rutledge, "Diode grids for electric beam stressing and frequency multiplication," *Int. J. Infrared and Millimeter Waves*, vol. 7, pp. 27–41, 1986.

[10] Y. I. Vorontsov and I. V. Polyakov, "Study of oscillatory in circuits with several series-connected tunnel diodes," *Radio Eng. Electron. Phys.*, vol. 10, pp. 758–763, May 1965.

[11] C. J. Madden, R. A. Marsland, M. J. M. Rodwell, D. M. Bloom, and Y. C. Pao "Hyperabrupt-doped GaAs nonlinear transmission line for picosecond shock-wave generation," *Appl. Phys. Lett.,* vol. 54, pp. 1019–1021, Mar. 1989.
[12] O. Boric, T. J. Tolmunen, E. Kollberg, and M. A. Frerking, "Anomalous capacitance of quantum well double-barrier diodes," *Int. J. Infrared and Millimeter Waves,* vol. 13, no. 6, pp. 799–813, 1992.
[13] E. R. Brown , T. C. L. G. Sollner, W. D. Goodhue, and C. D. Parker, "Millimeter-band oscillations based on resonant tunneling in a double-barrier diode at room temperature," *Appl. Phys. Lett.,* vol. 50, pp. 83–85, Jan. 1987.
[14] S. M. Sze, *Physics of Semiconductor Devices,* 2nd ed. New York: Wiley, 1981.
[15] C. E. Chang, P. M. Asbeck, K.-C. Wang, and E. R. Brown, "Analysis of heterojunction bipolar transistor/resonant tunneling diode logic for low-power and high-speed digital applications," *IEEE Trans. Electron. Devices,* vol. 40, no. 4, Apr. 1993.
[16] N. Kryroloff and N. Bogoliuboff, *Introduction to Non-Linear Mechanics.* Princeton: Princeton Univ. Press, 1943.

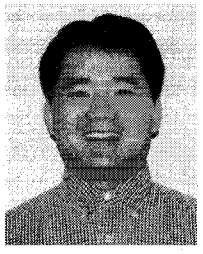

Runhua Sun (S'94) was born in Shanghai, China on August 31, 1965. He received the B.E. degree in electrical engineering from Shanghai University of Engineering Science, Shanghai, China in 1987, and the M.S. degree in applied mathematics from India University of Pennsylvania, in 1992.

Since 1992 he has been a Research Assistant in the Department of Electrical Engineering at the University of California, Los Angeles, where he is working toward the Ph.D. degree. His current research interests include excitation of series integrated RTD's and the modeling of the three terminal device.

Olga Boric-Lubecke (S'88), for a photograph and biography, see p. 976 of the April issue of this TRANSACTIONS.

Dee-Son Pan (M'89) received the B.S. degree in physics from Tsing-Hwa University, Taiwan, China in 1971, and the Ph.D. degree in physics from the California Institute of Technology in 1978.

He joined the faculty of the Electrical Engineering Department at UCLA as an Assistant Professor in 1977, where he is currently an Associate Professor. His current research interests are in device modeling, semiconductor physics and theoretical exploration of new devices. His recent works are in the area of enhancing the power of resonant tunneling diodes as a millimeter and submillimeter source, *p*-type quantum well device structures, and HBT devices.

Tatsuo Itoh (M'69–SM'74–F'82), for a photograph and biography, see p. 976 of the April issue of this TRANSACTIONS.